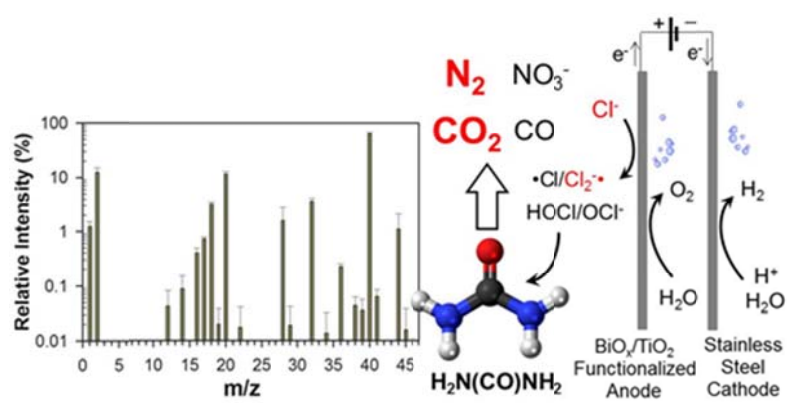


Chapter 2

UREA DEGRADATION BY ELECTROCHEMICALLY GENERATED REACTIVE CHLORINE SPECIES: PRODUCTS AND REACTION PATHWAYS



ABSTRACT

This study investigated the transformation of urea by electrochemically-generated reactive chlorine species (RCS). Solutions of urea with chloride ions were electrolyzed using a bismuth doped TiO₂ (BiO_x/TiO₂) anode coupled with a stainless steel cathode at applied anodic potentials (E_a) of either +2.2 V or +3.0 V versus the normal hydrogen electrode. In NaCl solutions, the current efficiency of RCS generation was near 30% at both potentials. In divided cell experiments, the pseudo-first-order rate of total nitrogen decay was an order of magnitude higher at E_a of +3.0 V than at +2.2 V due to the generation of dichlorine radical (Cl₂^{·-}) ions. Quadrupole mass spectrometer analysis of the reactor head-space revealed that N₂ and CO₂ are the primary gaseous products of the oxidation of urea, whose urea-N was completely transformed into N₂ (91%) and NO₃⁻ (9%). The higher reaction selectivity with respect to N₂ production can be ascribed to a low operational ratio of RCS to N. The mass-balance analysis recovered urea-C as CO₂ at 77%, while CO generation most likely accounts for the residual carbon. In light of these results, we propose a reaction mechanism involving chloramines and chloramides as reaction intermediates, where the initial chlorination is the rate-determining step in the overall sequence of reactions.

2.1. INTRODUCTION

Urea is the most abundant nitrogen (N) carrier in human excreta,¹⁻³ and therefore is the dominant source of N in domestic wastewater. In spite of the relatively low toxicity of urea, there is a growing concern that excessive N loading from toilet wastewater is leading to the eutrophication of surface waters. Major cities located in sensitive coastal areas are experiencing algal blooms in estuary waters that appear to be correlated to nutrient loading from household septic systems.⁴ During transport through sanitary sewer systems, urea-N is readily converted to NH_4^+ -N via enzymatic hydrolysis by urease. In septic systems, the pH can rise to 9 due to the protonation of ammonia released during the enzymatic hydrolysis.⁵ Due to the heavy loading of N in human waste, various groups are exploring source separation in order to harvest the urine at a reduced volume before discharge into a large volume disposal system.² In this respect, one can envision an on-site method for removing the N loading due to urea and thus avoiding problems resulting from the extended storage of toilet wastewater. Current demands on total maximum daily load reductions may require decentralized wastewater treatment methods, due to limited options for expanding the capacity of centralized wastewater treatment plants. The Bosch-Meiser process used to produce urea also discharges wastewater loaded with residual urea (< 30% of products¹) and thus requires a direct urea treatment technology other than the methods of adsorption or biological treatment that are currently employed.⁶

When compared to biological nitrogen removal processes (nitrification or Anammox) for urine treatment whose hydraulic retention times range up to a few days,² electrochemical treatment can be an efficient way to accomplish urea degradation at

relatively fast reaction rates (retention time within a few hours^{6,7}). Operational flexibility and energy sustainability can also be achieved when using a renewable energy source (*e.g.*, photovoltaic-panel⁸). Botte and co-workers⁹⁻¹¹ investigated nickel (II) hydroxide based electro-catalysts to facilitate a direct electron transfer from urea-N to anodes operating in a strong alkaline solution (*e.g.*, 1 to 5 M of KOH). Other electrochemical systems have explored mixed metal oxide anodes based on RuO₂, IrO₂, and PtO₂ to treat urea (< 0.2 M) with near equi-molar amount of chloride ion.^{6,7,12,13} In these systems, free reactive chlorine (HOCl or OCl⁻) appeared to be the primary oxidant leading to urea degradation, while chloramines were often observed as reaction intermediates.¹²

There appears to be a reasonable consensus that N₂ and CO₂ are the eventual products during chlorination of urea,^{7,13} although there are reports of N₂O (nitrous oxide) as a final N-containing product.¹⁴ However, little data can be found on the exact speciation of the potential array of gaseous products. On the other hand, we recently demonstrated that electrochemically generated chlorine radicals can rapidly reduce the chemical oxygen demand in domestic wastewater.¹⁵ In this case, the reactive chlorine species (RCS) is used as a collective term for the sum of free chlorines and chlorine radicals such as the chlorine atom (Cl[·]) and chlorine radical anion (Cl₂^{·-}).

With these considerations in mind, we now report on the details of N transformation during urea degradations via RCS generated on hetero-junction anodes functionalized with bismuth-doped titanium dioxide (BiO_x/TiO₂). Parallel analyses of products generated in the aqueous phase and gas phase allowed for mass and charge balance determinations of the nitrogenous and carbonaceous species. The effects of applied

anodic potential (E_a) on the rates of total nitrogen (TN) decay and products formation were also explored in order to assess the detailed roles of chlorine radicals during urea oxidation. The degradation of urea by electrochemically generated RCS seems to resemble the ‘chemical (most often using NaOCl)’ chlorination mechanisms¹⁴ (the process used to investigate the formation of chlorinated byproducts in swimming pools). However, we note that the differences in operational molar ratios of RCS to N as well as the chlorine radical generation rates change the kinetic parameters and the selectivity towards the final products in the electrolytic urea degradation.

2.2. EXPERIMENTAL SECTION

2.2.1. Preparation of BiO_x/TiO₂ Anode and Electrolysis Cell. In a typical preparation,^{15,16} Ti metal sheets (0.5 mm thick, pretreated by sand-blasting, degreasing, and etching) were doubly coated sequentially with mixed metal oxide layers by repetitive thermal decomposition of Ir/Ta solution (73 mM H₂IrCl₆ and 27 mM TaCl₅ in 4 M HCl; anneal at 525 °C), Sn/Bi solution (225 mM SnCl₄ and 12.5 mM Bi₂O₃ in 0.5 M HCl; at 425 °C), Ti/Bi slurry (*ca.* 300 mM Bi-doped TiO₂; at 250 °C), and Ti/Bi solution (225 mM Ti-Glycolate complex and 25 mM bismuth citrate in 75 mM NH₄OH; at 425°C).

Single compartment electrolysis cells (working volume of 60 mL) were prepared using a BiO_x/TiO₂ anode and stainless steel cathode pair (3 × 2 cm², 5 mm gap) with a Ag/AgCl/Sat. KCl reference electrode (BaSi Inc., USA) whose Vycor® glass tip was 2 mm apart from the anode center. For divided cell configuration, a Pt wire encapsulated in a tube with Vycor® glass frit separator was used as a cathode. A schematic diagram of

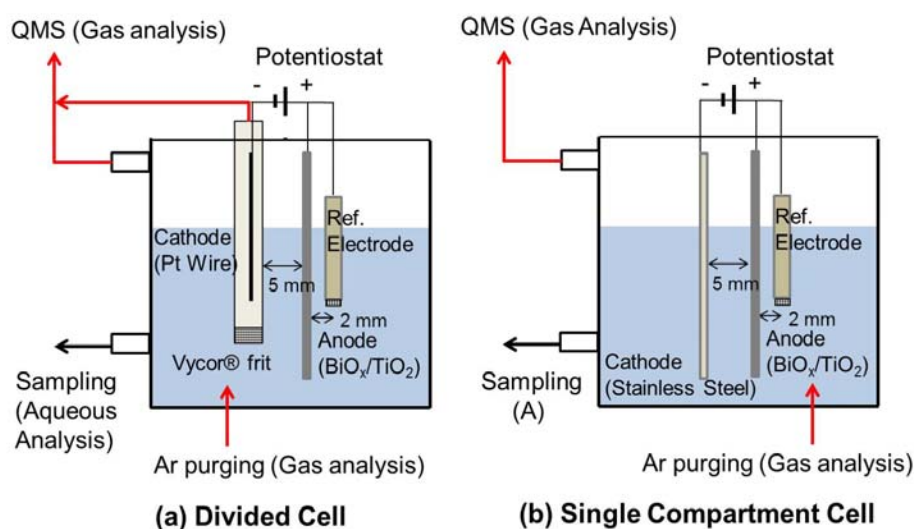


Figure 2.1. Schematic diagram of electrolysis cells (working volume: 60 mL) used in this study.

each electrolysis cell is shown in Figure 2.1. The frit separator reduces interferences of cathodic reactions to estimate more reliable kinetic parameters, while an increased electrical resistance of the divided cell decreases the response current density (J) at a given E_a . All electrochemical experiments were performed under potentiostatic conditions driven by a SP-50 potentiostat (Bio-Logics, USA).

2.2.2. Potentiostatic Electrolysis of NaCl Solutions with or without Urea. The rate and current efficiency of RCS generation were estimated in the single compartment cell with 50 mM NaCl solutions. The RCS evolution rates were measured in terms of total chlorine (Cl_{DPD}) concentrations at a fixed time interval (2 min) three times. The relatively short reaction duration (6 min) was intended to minimize the oxidation or reduction of RCS, which would cause a non-linear increase of [RCS] with time.^{16,17} These experiments were repeated with E_a varying from 1.5 to 3.0 V versus the normal hydrogen electrode (NHE).

The current efficiency for the RCS generation (η_{RCS}) was estimated by the following equation:

$$\eta_{RCS} = \frac{2VF d[Cl_{DPD}]}{I dt} \quad (2.1)$$

where, V is electrolyte volume (0.06 L), F is Faraday constant (96485.3 C mol⁻¹), $[Cl_{DPD}]$ is the concentration of RCS (M), I is current (A), and t is electrolysis time (sec).

The electrochemical urea degradation experiments were performed in a divided cell (E_a : 2.2 V or 3.0 V NHE, 3 h) or in a single compartment cell (E_a : 3.0 V NHE, 6 h). The reaction solution contained 41.6 mM (2.5 g L⁻¹) of urea in the presence of 50 mM NaCl (electrical conductivity: 5.6 ± 0.1 mS cm⁻¹). The initial [urea] was in accordance with a recipe for synthetic urine¹⁸ assuming 10-fold dilution by flushing. The molar ratio of urea-N to Cl⁻ (close to 1.7) was compatible with operational ranges in analogous literature,^{6,12} while it was less than half of the observed ratios for fresh urine.² We rationalize the low urea-N/Cl⁻ ratio by the scenario either of moderate storage before treatment (decreasing [urea]) or reuse of treated effluent as flushing water (increasing [Cl⁻]). Urea solutions with 50 mM Na₂HPO₄ (7.4 ± 0.1 mS cm⁻¹) were also tested in the divided cell as control experiments, to evaluate urea oxidation by a direct electron transfer from urea to the semiconductor anode. Small aliquots of electrolyte were sampled periodically to monitor the speciation of aqueous-phase N. Gaseous products in the reactor headspace were analyzed by HPR-20 gas analysis system (Hidden Analytical, USA) with a heated quartz inert capillary inlet under continuous purging of Ar gas (*ca.* 7 mL min⁻¹).

2.2.3. Analytical Methods. The pH, conductivity and electrical resistance of solutions before and after the electrolysis were determined using a pH meter (Mettler Toledo, USA), a conductivity meter (VWR International, USA), and the current interruption function of the potentiostat with a current bias of 200 mA, respectively. The [urea] was determined using a hydrolysis method employing Jack Bean Urease as described previously.¹⁶ However, the measured values of [urea] were reliable only for the control experiments due to interferences of RCS with urease activity.²⁰ The principal ions of interest (Cl^- , ClO_3^- , NO_2^- , NO_3^- , NH_4^+) were quantified by DX-500 ion chromatography system (Dionex, USA), equipped with the anion-exchange column Ionpac AS 19 and the cation-exchange column Ionpac CS 16. [TN] were determined using low range (0.5 to 25 mg N L⁻¹) TN reagent kits (Hach, USA) according to absorbance at 420 nm in the UV-VIS spectrophotometer (Agilent, USA) after digestion. The Cl_{DPD} was measured with DPD (N,N-diethyl-p-phenylenediamine)/KI reagents (Hach, USA) based on the absorbance at 530 nm. It has been reported that, in urea chlorination, the Cl_{DPD} accounts for chlorinated urea species as well as inorganic chloramines.²¹ Analogous measurements with DPD reagents (Hach, USA) were performed to quantify the fraction of free chlorine in the Cl_{DPD} . The gaseous products underwent 70 eV electron impact ionization, and fragments (m/z 1 to 300) were analyzed using a quadrupole mass spectrometer (QMS) in a vacuum ($< 5.0 \times 10^{-6}$ Torr) generated by a turbo pump. The volume percent in the headspace gas was assumed to be directly proportional to the ion current measured by the QMS. Quantification of the gases of interest was based on the relative ion current intensities of characteristic m/z (14 for N_2 , 44 for CO_2) and the volumetric flow rate of total gaseous products measured with a mass flow-meter (Bronkhorst, USA). The limit of

detection, defined as three times the standard deviation of the relative ion intensities under injection of blank gas (Ar), was estimated to be *ca.* 100 ppm for m/z 1 to 46 (except fragments from Ar) and 1 ppm for m/z 47 to 300. Additional details are given in Supporting Information.

2.3. RESULTS AND DISCUSSION

2.3.1. RCS Generation on BiO_x/TiO₂ Anode. Figure 2.2 shows the RCS generation profiles obtained with the BiO_x/TiO₂ anode in 50 mM NaCl solutions with circum-neutral pH. The Cl_{DPD} in absence of N compounds accounts for RCS, although it should exist predominantly as free chlorine due to the short life of the chlorine radicals. Cl⁻ oxidation in terms of the specific RCS generation rate monotonically increased along with J as the E_a increased from 1.5 to 3.0 V NHE (corresponding to cell voltages ranging from 2.5 to 6.0 V). The dependency of J on E_a was nominally linear in dilute chloride solutions due to resistances between anode and the reference electrode; *i.e.*, iR -drop attenuates the exponential response of J described by the Butler-Volmer formulation.¹⁵ The η_{RCS} was below 10% at E_a of 1.5 V NHE (slightly higher than the redox potential of the Cl₂/Cl⁻ couple), and increased to 24 – 30% at higher potentials. The losses in current efficiency (> 70%) can be dominantly ascribed to the oxygen evolution reaction. In the case of the mixed metal oxide (BiO_x/TiO₂) anode, the surface titanol (*i.e.*, >TiOH) groups provide the active sites for surface hydroxyl radical formation, while the redox transitions of BiO_x (III/V) or underlying IrO_x (IV/VI) serve as electron sinks.¹⁵

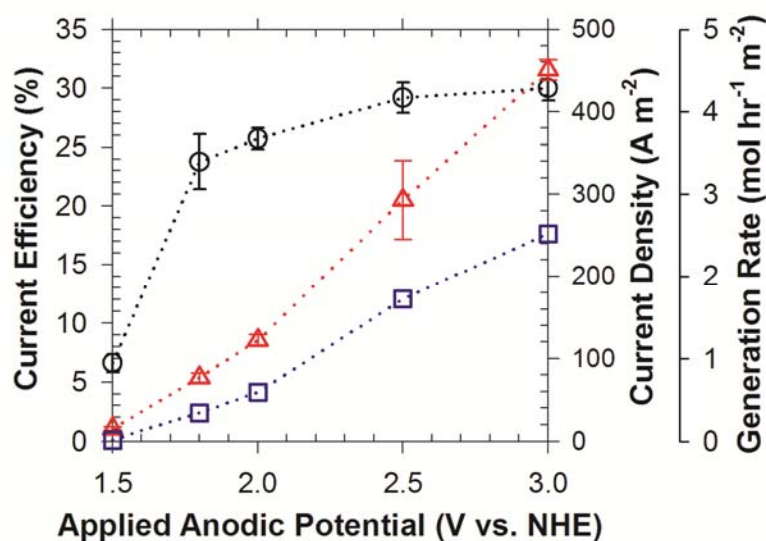


Figure 2.2. Current efficiency (circle) and rate (square) of reactive chlorine generation together with current density (triangle) on average as functions of applied anodic potential during potentiostatic electrolysis of 50 mM NaCl solutions in single compartment cell; anode: BiO_x/TiO₂ (6 cm²), cathode: stainless steel (6 cm²). Error bars represent the standard deviations for three samples collected with 2 min intervals.

In this study, the current efficiencies were quasi-constant at potentials higher than 1.8 V NHE. These observations have the following implications; i) the power efficiency for RCS generation should decrease along with E_a , and ii) one can expect a linear dependence of the RCS generation rate on J under the experimental conditions of this study.

2.3.2. Aqueous and Gaseous Products Formed During Urea Degradation. Figure 2.3 shows the transformation of nitrogen during electrolysis of urea solutions with Cl⁻ in the divided cell. Urea degradation was negligible in a phosphate electrolyte or under E_a of

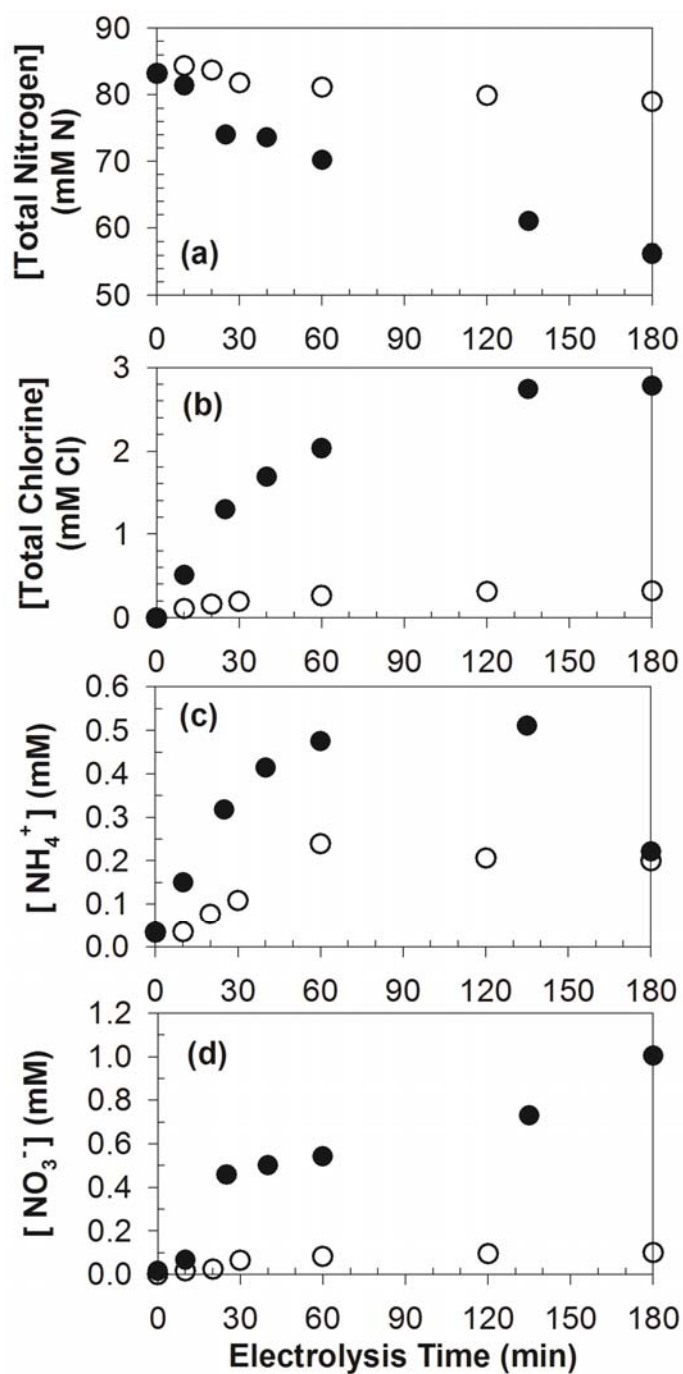


Figure 2.3. Time profiles of (a) total nitrogen, (b) total chlorine (Cl_{DPD}), (c) NH_4^+ , and (d) NO_3^- concentration during potentiostatic electrolysis of 41.6 mM urea solutions with 50 mM Cl^- (60 mL) in divided cell; anode: $\text{BiO}_x/\text{TiO}_2$ (6 cm^2), cathode: Pt wire in frit separator, applied anodic potential: 2.2 V NHE (empty circle), 3.0 V NHE (filled circle).

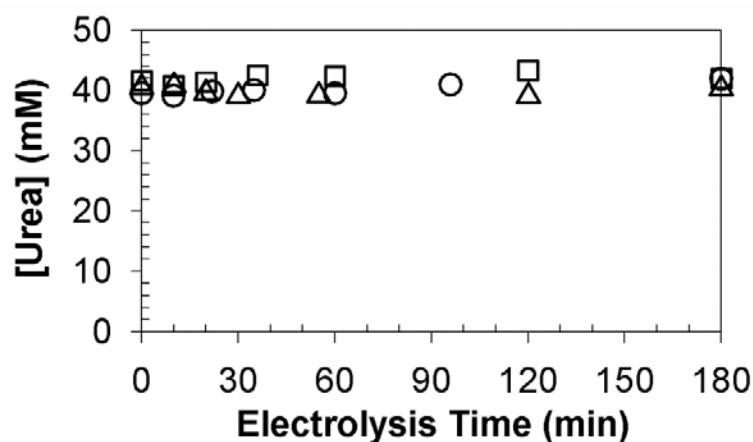


Figure 2.4. Time profiles of urea concentration during control electrolysis of 41.6 mM urea solutions in a divided cell; E_a : (circle) 2.2 V NHE with 50 mM Na₂HPO₄, (triangle) 3.0 V NHE with 50 mM Na₂HPO₄, (square) 1.3 V NHE with 50 mM NaCl, anode: BiO_x/TiO₂ (6 cm²), cathode: Pt wire in frit separator.

1.3 V NHE in a chloride background (Figure 2.4). These results indicate that a direct electron transfer from urea-N to surface sites on the anode is negligible. The [Cl_{DPD}] was consistently below the detection limit in these control experiments so that a potential interference of reactive oxygen species could be ruled out in subsequent electrolysis experiments. We recently reported^{15,16} that, on the BiO_x/TiO₂ anode, the surface bound hydroxyl radicals are readily quenched by redox transitions of Bi(III/IV) to form higher oxides which prefer oxygen evolution to reactive oxygen species generation.¹⁶

The aqueous products from the electrolytic degradation of urea included NH₄⁺, NO₃⁻, chloramines (*i.e.*, NH₂Cl, NHCl₂, NCl₃), and chlorinated urea. Concentrations of free chlorine were below the detection limit, indicating that the chloramines and chloramides primarily account for the measured Cl_{DPD}. The time profiles of the aqueous products were compatible with the previous reports on chemical urea oxidation by NaOCl.¹⁴ These

suggested that urea is sequentially chlorinated to tetrachlorourea which is oxidized further to produce CO_2 and inorganic chloramines.^{3,14} The reversible hydrolysis of chloramines will yield NH_4^+ depending on the pH and the $[\text{RCS}]$.^{22,23} In addition, the inorganic chloramines are believed to undergo base catalyzed disproportionation to produce gaseous N as in breakpoint chlorination²⁴, while NHCl_2 is further oxidized to NO_3^- .²² The overall chemical reaction is known to be limited by the first chlorination step of urea, whereas subsequent reactions proceed at much faster rates.^{3,14}

At circum-neutral pH, the nominal second-order rate constant for the reaction of urea with free chlorine was determined to be $0.63 \text{ M}^{-1} \text{ s}^{-1}$.²⁵ In contrast, the bimolecular reaction between NHCl_2 and NCl_3 has a rate constant of $5.6 \times 10^3 \text{ M}^{-1} \text{ s}^{-1}$,²² while the reaction between NH_2Cl and NCl_3 has a bimolecular rate constant of $1.4 \times 10^2 \text{ M}^{-1} \text{ s}^{-1}$. In this study, the rate-limiting step in the reaction sequence was found to be the initial reaction between urea and RCS as well. The evolution of gaseous nitrogen appeared to correspond directly to the 'urea + RCS \rightarrow reaction intermediates', since the rate of urea degradation was correlated with the rate of TN decay. The sums of Cl_{DPD} , NH_4^+ , and NO_3^- concentrations were much smaller than the reduced TN concentrations, which in turn should account for the production of gaseous N species.

Figure 2.5 shows the relative intensities of the ion fragments for the gas products in the single compartment cell experiments. Based on the NIST/EPA/NIH Mass Spectral Library (NIST11), the major peaks in the mass spectrum (m/z 1 to 46) consisted of H_2 (m/z 1 and 2), O_2 (m/z 34, 32 and 16), H_2O (m/z 16 to 19), CO_2 (m/z 44 to 46, 28, 22, 16,

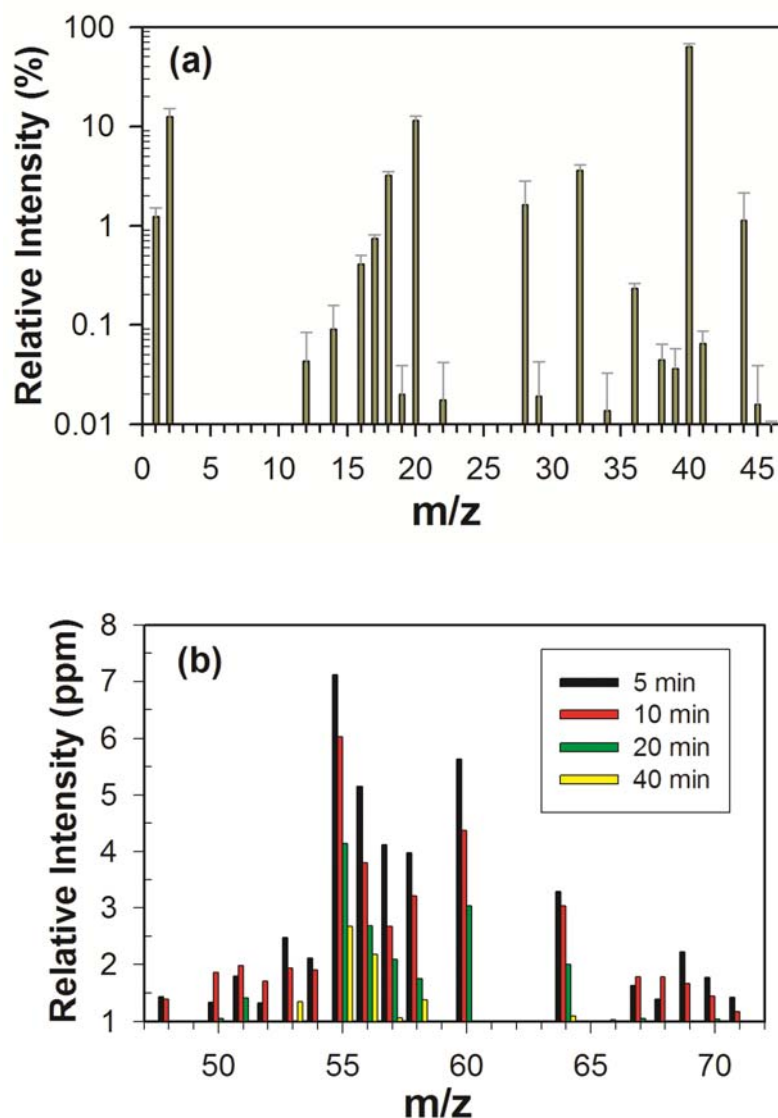


Figure 2.5. Relative intensities of ion fragments in quadrupole mass spectrometer analysis of gaseous products during potentiostatic electrolysis of 41.6 mM urea solutions with 50 mM Cl^- (60 mL) in single compartment cell; anode: $\text{BiO}_x/\text{TiO}_2$ (6 cm^2), cathode: stainless steel (6 cm^2), applied anodic potential: 3.0 V NHE. Error bars represent the standard deviations of periodic measurement (detection interval: 1 min).

and 12), N₂ (m/z 29, 28 and 14), and Ar (m/z 40, 38, 36 and 20). From the mass spectral analysis, N₂ appears to be the principal gaseous N product in urea degradation. A negligible signal at m/z 30 (*i.e.*, N₂O) indicates that nitrous oxide is a trace-level product. On the other hand, the ratios of mean signal intensities from H₂ to those from O₂ were much higher than the stoichiometric ratio in water splitting (2:1). This implies that non-stoichiometric water splitting was taking place. Heterogeneous Cl⁻ oxidation appears to be the main scavenging reaction of oxygen generation at the electrode surface.²⁶ This process in turn increases the bulk solution pH during electrolysis. Considering that the intensity of m/z 15 was below the detection limit, a stripping of dissolved NH₃ is not apparent due to the low [NH₄⁺] in solution (*vide infra*).

2.3.3. Urea Degradation Kinetics in a Divided Cell. As an extension of our recent work,¹⁵ we argue that the electrochemical transformation of urea is accelerated by generation of chlorine radical species. The mean current density at applied potential, E_a , at 3.0 V NHE (83 A m⁻²) was 3.6 times higher than at 2.2 V NHE (23 A m⁻²). If the heterogeneous RCS generation is rate limiting, then the formation rates of NO₃⁻ or N₂ should be proportional to J , given the comparable values of η_{RCS} as shown in Figure 2.2. However, the apparent pseudo first-order decay rate of TN (k_{TN}) in Figure 2.3a was estimated to be $4.4 \times 10^{-6} \text{ s}^{-1}$ and $4.0 \times 10^{-5} \text{ s}^{-1}$. The increase of k_{TN} with E_a (9 times) exceeds the proportionality as predicted by the values of J (3.6 times). In addition, the initial rates of Cl_{DPD} evolution in Figure 2.3b increased by more than an order of magnitude under the higher potential bias ($5.5 \times 10^{-8} \text{ M s}^{-1}$ and $7.8 \times 10^{-7} \text{ M s}^{-1}$, respectively, by linear regression to the initial three data points).

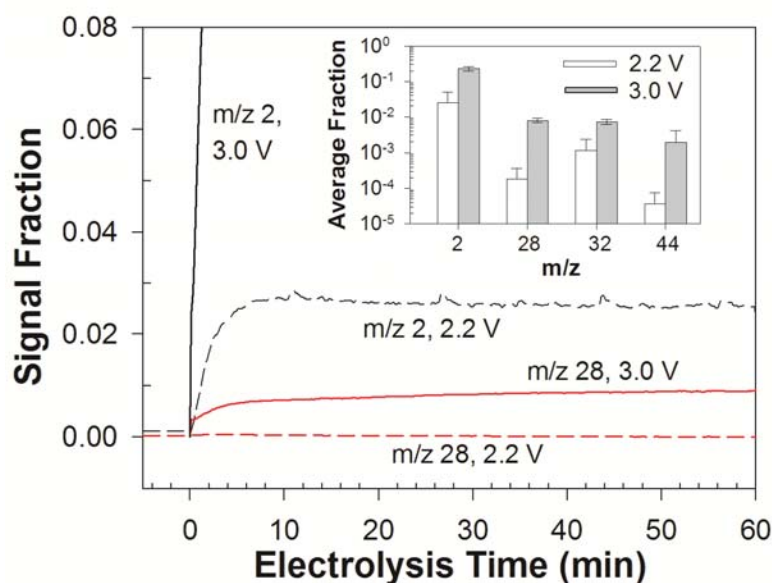


Figure 2.6. Time profiles of relative intensities for ion fragments m/z 2 and 28 in quadrupole mass spectrometer analysis during potentiostatic electrolysis of 41.6 mM urea solutions with 50 mM Cl^- (60 mL) in divided cell; E_a : 2.2 V NHE (dashed line), 3.0 V NHE (solid line), anode: $\text{BiO}_x/\text{TiO}_2$ (6 cm^2), cathode: Pt wire in frit separator. Inset figure shows the relative intensities on average for ion fragments m/z 2, 28, 32, 44 for the initial 1 h.

The measurement of gaseous products in a divided cell (Figure 2.6) further supports the enhanced N_2 generation with increasing applied potential. When the E_a was set at 3.0 V NHE, mass fragments appeared immediately at m/z 2 (H_2), 32 (O_2), and m/z 28 (N_2 and CO_2). When the potential was set at 2.2 V NHE, in contrast, the generation of N_2 and CO_2 were minimized, while the oxygen/hydrogen signals were found to be in good agreement with the current density. These combined observations demonstrate that the urea degradation is limited by the homogeneous reaction between urea and RCS.

The chemical reaction network for the electrochemical oxidation of urea mediated by RCS can be summarized in terms of three kinetically significant steps. They are i)

heterogeneous RCS generation, ii) the initial reactions of RCS with urea, and iii) subsequent oxidation reactions involving the initial reaction intermediate (expressed as Cl_{DPD}) to produce N_2 . Given this simplification, the governing equations can be written as eq 2.2 and 2.3:

$$-\frac{d[\text{TN}]}{dt} = 2 \left(\sum_i k_{1i} [\text{RCS}_i] \right) [\text{Urea}] = k_{\text{TN}} [\text{TN}], \quad k_{\text{TN}} = \sum_i k_{1i} [\text{RCS}_i] \quad (2.2)$$

$$\frac{d[\text{Cl}_{\text{DPD}}]}{dt} = k_{\text{TN}} [\text{Urea}] - k_2^* [\text{Cl}_{\text{DPD}}], \quad k_2^* = \sum_i k_{2i} [\text{RCS}_i] \quad (2.3)$$

where k_{1i} and k_{2i} represent the second order rate constants for the reaction of reactive chlorine species i (RCS_i) with urea and reaction intermediates (Cl_{DPD}), respectively. The presence of the most abundant reaction intermediates should justify the usage of Cl_{DPD} as an effective summation term. The pseudo-steady-state concentrations of RCS_i allow for the introduction of collective constants, k_{TN} and k_2^* . Eq 2.3 corresponds to the situation in which the initial oxidation of urea is the slow rate-determining step compared with the following steps. In this case, monochlorourea was presumed to be the primary Cl_{DPD} , since sequential chlorination would provide more acidic amido-N moieties which undergo more facile hydrogen abstraction.¹⁴ Use of the divided cell reactor should minimize other RCS-quenching reactions, such as cathodic RCS reduction and anodic chlorate formation. For example, the final chlorate concentrations in the divided cell experiments were less than 1% of the initial chloride concentration, primarily owing to the relatively low current density (*vide infra*). The above set of simplified equations describes the $[\text{TN}]$ versus time in terms of a simple pseudo first-order decay profile

(when $2[\text{Urea}] \sim [\text{TN}]$). Non-linear regressions to the observed $[\text{Cl}_{\text{DPD}}]$ predicted k_2^* of $5 \times 10^{-4} \text{ sec}^{-1}$ at 2.2 V NHE and $7 \times 10^{-4} \text{ sec}^{-1}$ at 3.0 V NHE.

The bulk solution pH increased up to 9.5 after the divided cell experiments, due to the non-stoichiometric water splitting. The pK_a of HOCl (7.5) and the solution pH suggest that OCl^- would be the dominant oxidant at the E_a of 2.2 V NHE. However, an acidic environment in anode vicinity would allow for contributions of Cl_2 , which was reported to have higher reactivity to urea than HOCl and OCl^- .¹⁴ Although our simplified kinetic approach could not provide rate constants of individual RCS, the collective kinetic parameters (k_{TN} , k_2^*) qualitatively indicate a shift in RCS speciation. The iR -compensated anodic potential at E_a of 3.0 V NHE (Table 2.1) was greater than the equilibrium potential needed to liberate ‘free’ chlorine radical species ($\text{Cl}\cdot/\text{Cl}_2\cdot^-$).^{15,26} In this case, the urea degradation would be initiated by hydrogen abstraction or electrophilic addition of chlorine atom by radicals, whose bimolecular rate coefficients are expected to be much higher than those by free chlorine. Considering the $[\text{Cl}_2\cdot^-]/[\text{Cl}\cdot]$ ratio with $[\text{Cl}^-]$

Table 2.1. The ohmic drop compensated anodic potential ($E_a - iR$) and current density (J) on average during the electrolysis of 41.6 mM urea solutions with 50 mM chloride (60 mM) under variable cell types and applied potentials (E_a).

Cell Type	E_a (V, NHE)	$E_a - iR$ (V, NHE)	J (A m^{-2})
Divided	2.2	1.73 (3.1)	23.8 (20)
	3.0	2.24 (4.7)	83.3 (14)
Single Compartment	3.0	2.05 (3.5)	458 (7.5)

of 50 mM (7×10^3 using K_{eq} of $1.4 \times 10^3 \text{ M}^{-1}$), the dichlorine radical anion is expected to be the major radical species under our operating conditions.²⁶ The reactivity between urea and $\text{Cl}_2\cdot^-$ has not been reported in literature. As a reference, apparent rate constants of free chlorine reacting with primary amines are in the order of $10^4 \text{ M}^{-1} \text{ s}^{-1}$,²⁵ while the reactivity of dichlorine radical has been reported up to $10^7 \text{ M}^{-1} \text{ s}^{-1}$.²⁷ Nevertheless, the increases of k_{TN} and k_2^* with E_a were within similar orders of magnitude, indicating that the roles of free chlorine should not be ignored even under the radical generation. The $\text{Cl}_2\cdot^-$ radicals in the aqueous phase are expected to be rapidly disproportionated to free chlorine with diffusion-limited second-order rate constants ($> 10^9 \text{ M}^{-1} \text{ s}^{-1}$).²⁶

2.3.4. Urea Transformation Characteristics in Single Compartment Cell. Additional experiments were performed in a single compartment cell with a paired electrode module (E_a : 3.0 V NHE) to investigate the transformation efficiency in a practical setup. As shown in Figure 2.7, the $[\text{Cl}_{\text{DPD}}]$ followed a typical profile of the breakpoint chlorination; *i.e.*, an initial rise with chloramines/chloramides production, subsequent decrease by chloramine disproportionation to N_2 until the breakpoint is achieved after 4 h, followed by subsequent further increase of free chlorines. Free chlorine concentration was inappreciable until 4 h of electrolysis, while almost superimposable to $[\text{Cl}_{\text{DPD}}]$ for the last sample (after 6 h). $[\text{NH}_4^+]$ showed a peak (0.7 mM) at 3 h of electrolysis and decayed to be negligible along with the dismutation of chloramines. Consequently, the initial urea-N was almost completely transformed into nitrate and N_2 after 6 h, where the residual $[\text{TN}]$ ($\sim 8 \text{ mM}$) roughly coincided with the $[\text{NO}_3^-]$. Figure 2.7c shows molar flow rate of N_2 and CO_2 quantified by volumetric gas flow rate and the observed QMS output signals of

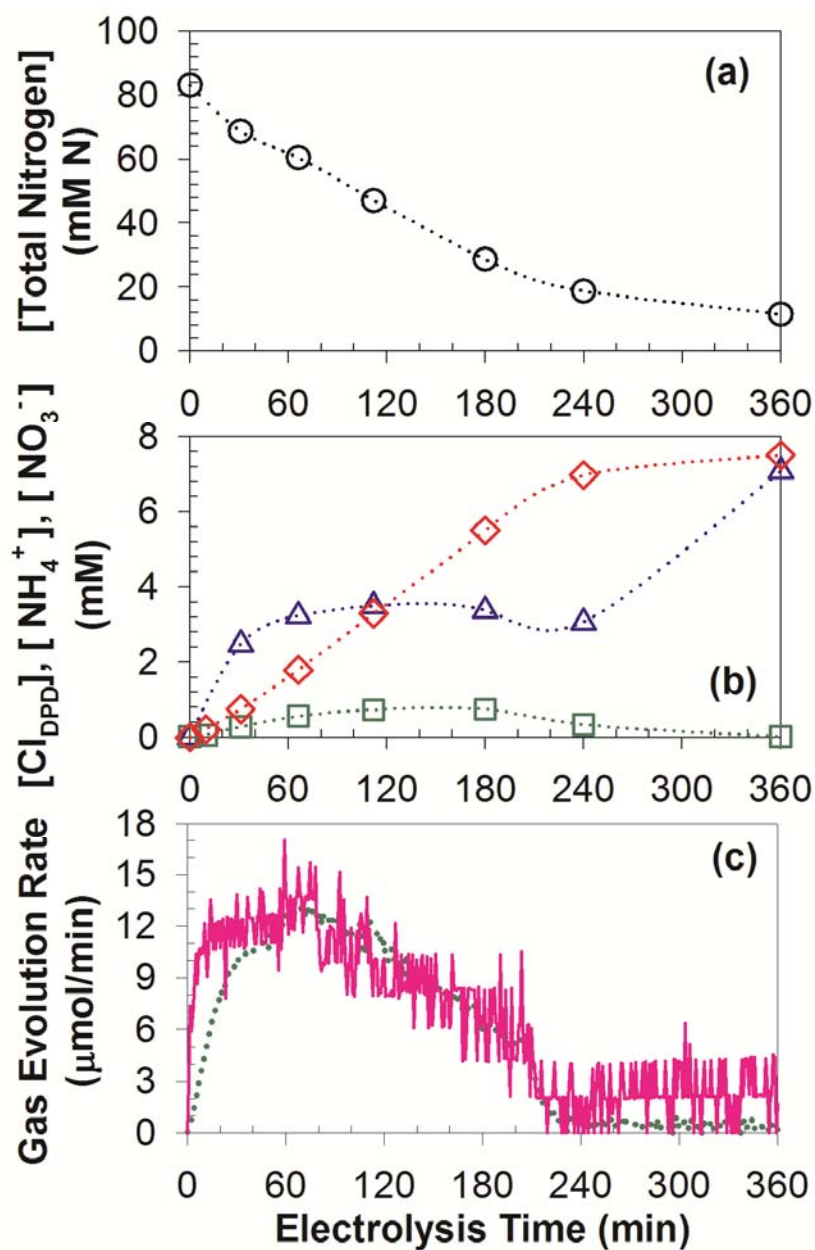


Figure 2.7. Time profiles of total nitrogen (circle), total chlorine (triangle), ammonium (square), and nitrate (diamond) concentration together with molar flow rate of N_2 (solid line) and CO_2 (dotted line) during potentiostatic electrolysis of 41.6 mM urea with 50 mM Cl^- (60 mL) in single compartment cell; anode: $\text{BiO}_x/\text{TiO}_2$ (6 cm^2), cathode: stainless steel (6 cm^2), applied anodic potential: 3.0 V.

characteristic m/z ratios. The generation rates of these major gas products followed exponential relationships as predicted by the pseudo first-order kinetic analysis. A mass balance analysis for N indicated that 5 mmol of urea N is transformed into 4.56 mmol N as N_2 (91%) and 0.45 mmol N as NO_3^- (9%). The total amount of CO_2 in the gas products was quantified to be 1.92 mmol, somewhat smaller than the carbon input (2.50 mmol). Furthermore, the signal response at m/z 28 was greater than the expected sum by the characteristic m/z signals of N_2 and CO_2 . These observations indicate that CO is being formed as a minor carbon-containing product.

Greater selectivity for gaseous N species than for NO_3^- has been reported previously in the electrochemical oxidation of urea^{5,7,8} and NH_4^+ ^{23,28}. A lower selectivity toward NO_3^- is beneficial with respect to the chlorine demands exerted by urea which, in turn, should be proportional to the energy consumption in electrochemical systems. Stoichiometric chlorine demands range from 3 to 8 mol mol⁻¹ of Cl_2 /urea depending on the selectivity. On the contrary, chemical urea chlorinations^{3,14} under initial chlorine dosage exceeding 1 mol mol⁻¹ of Cl_2 /urea have reported much higher relative yields of NO_3^- (up to 40%). The nitrate yields appeared to monotonically increase with the applied chlorine dosage (3 ~ 10 mol mol⁻¹ of Cl_2 /urea), with observed chlorine demands up to 5 mol mol⁻¹ of Cl_2 /urea.³ The NO_3^- is believed to be produced from dichloramine oxidation by RCS,^{12,22} which should be more sensitive to the RCS concentration than N_2 generation reactions among chloramines. Therefore, a low yield for NO_3^- in the electrolytic urea degradation can be attributed to a presumable low RCS/urea ratio with pseudo steady-state concentration of RCS. The present results have some practical implications for control of selectivity towards N_2 and NO_3^- in treatment of N-containing wastewater. The

electrochemical urea chlorination with greater selectivity to N_2 can be broadly deployed for remediation of N-rich wastewater (black water from toilet and livestock industry, landfill leachate), aiming at N loading reduction. When focusing on N recovery for fertilizer production, increasing J is expected to elevate the nitrate yield,²⁹ which is consistent with our observations in this study. In the divided cell experiments under lower J (Figure 2.3), the nitrate yield was estimated to be 3.7% at E_a of 3.0 V NHE. An external RCS generation in a multi-component reactor with flow regulation can be another feasible approach to enhance the nitrate yield.

Despite the higher TN decay rate with respect to the electrolysis time, the magnitude of the TN decrease per unit of passed charge was lower in the single compartment cell than in the divided cell (Figure 2.8) at a given E_a . The lower current efficiency in the absence of the fritted-glass separator can be attributed to quenching reactions of RCS such as cathodic reversion to Cl^- and further oxidation to ClO_3^- .^{15,16} When the total passed charge (5936 C) in the single compartment cell experiment was compared with the theoretically required charge for the observed products, the current efficiency was estimated to be 22% for N_2 (6 e^- transfer per molecule), 5.9% for NO_3^- (8 e^-), 7.0% for ClO_3^- (6 e^-), and 1.4% for residual Cl_{DPD} (2 e^-), respectively. The sum of anodic current efficiency (36%) slightly exceeds the η_{RCS} measured in NaCl solutions (30%, Figure 2.2), supporting the hypothetic CO generation as an electron source. The nominal energy consumption in the single compartment cell electrolysis (6 h) was 186 $kJ L^{-1}$, considerably greater than in biological nitrogen removal process (*ca.* 5 $kJ L^{-1}$).² The relatively intensive energy requirement of electrochemical approaches can be mitigated

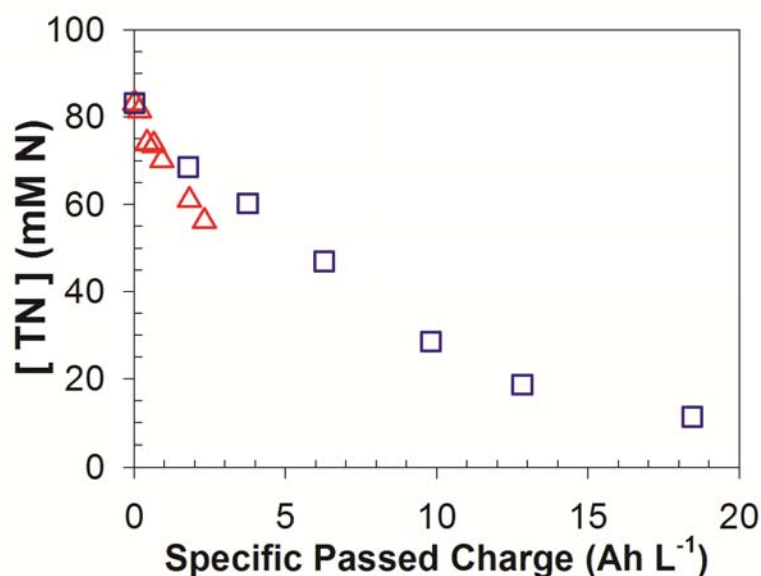


Figure 2.8. Total Nitrogen (TN) concentrations as functions of specific passed charges during potentiostatic electrolysis of 41.6 mM urea solutions with 50 mM Cl⁻ (60 mL) in a divided (triangle) and single compartment (square) cell; E_a : 3.0 V NHE, anode: BiO_x/TiO₂ (6 cm²).

by their compatibility with renewable energy sources. For example, our recent report¹⁵ estimated that about 3.5 m² of a photovoltaic panel can achieve break-even energy balance in an electrochemical system designed to treat wastewater from a community toilet for 30 users.

2.3.5. Byproducts Formation. The electrolytic urea degradation in the single compartment cell showed that ClO₃⁻ is a dominant aqueous-phase byproduct, most likely formed by the heterogeneous oxidation of free chlorine (HOCl and ClO⁻).^{15,16} The [ClO₃⁻] increased almost linearly with the electrolysis time (or specific amount of charge passed) until the breakpoint, after which the generation was accelerated (Figure 2.9). The [ClO₃⁻] profiles versus specific passed charges did not show a noticeable deviation between the

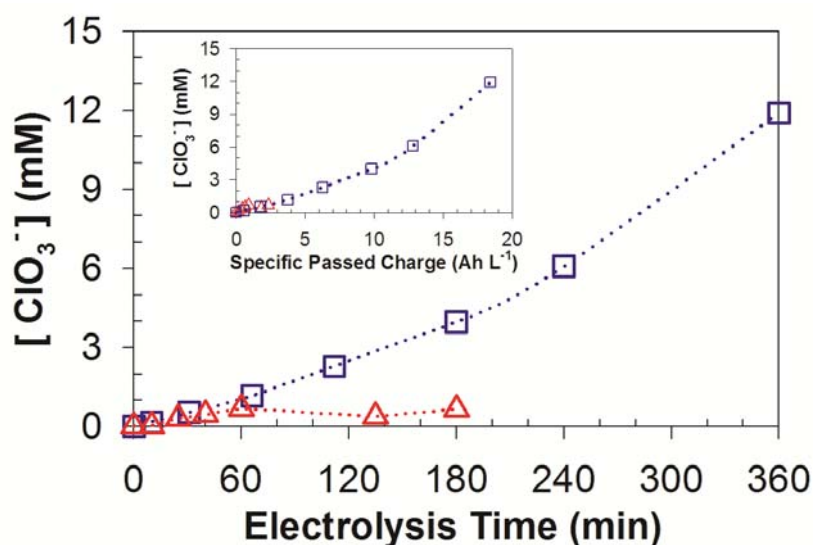


Figure 2.9. Evolutions of ClO_3^- concentration as functions of electrolysis times and (inset) specific passed charges during potentiostatic electrolysis of 41.6 mM urea solutions with 50 mM Cl^- (60 mL) in a divided (triangle) and single compartment (square) cell; E_a : 3.0 V NHE, anode: $\text{BiO}_x/\text{TiO}_2$ (6 cm^2).

single component and divided cell. Therefore, the current efficiency of chlorate production is likely more sensitive to the relative amount of potential electron donors to RCS, than it is to J . In this study, the ClO_3^- was a stable byproduct without an appreciable concentration of perchlorate ion (ClO_4^-). The ClO_4^- has often been observed by oxidation of ClO_3^- on a boron doped diamond anode.²⁹ In light of the standard redox potential of the $\text{ClO}_4^-/\text{ClO}_3^-$ couple (1.19 at pH 0), the production of ClO_4^- is likely to be kinetically limited in our operational condition.

This study could not clearly identify the volatile chlorinated compounds other than NH_2Cl from a time lapse QMS measurement (detection interval: 1 min) of the gas products (Figure 2.5b). The molecular ion signals from m/z 72 to 300 were always lower than the limit of detection (1 ppm). Weak peaks at m/z 51 and 53 could be assigned to

$\text{NH}_2^{35}\text{Cl}$ and $\text{NH}_2^{37}\text{Cl}$. Their maximum ion intensities were always observed at the start-up and then decayed to below the detection limit within 1 h. The peak cluster at m/z 48 to 52 and 64 corresponded to chloromethane ($\text{CH}_3^{35}\text{Cl}$ and $\text{CH}_3^{37}\text{Cl}$), chloroethane ($\text{C}_2\text{H}_5^{35}\text{Cl}$), and their fragments. The other detected signals could not be explained in terms of the chlorinated compounds in the database, although they most likely followed fragmentation characteristics of condensed alkanes and alkenes (C_4H_8 , C_4H_{10} , C_5H_{10} , and C_5H_{12}), methyl isocyanate (CH_3NCO), oxalic acid ($\text{H}_2\text{C}_2\text{O}_4$), and acetic acid (CH_3COOH). However, these compounds with reduced oxidation states of carbon are not likely to evolve from urea chlorination. Despite a lack of mass spectral data in the library, we suspect that these peak clusters with minor fractions might be ascribed to chlorinated carbamic acids or chlorinated hydrazines as potential reaction intermediates (*vide infra*).

Volatile disinfection byproducts reported in chlorinated swimming pools³⁰⁻³² include inorganic chloramines, CNCl , CHCl_3 , nitriles, and halonitroalkanes, depending on precursor composition and applied Cl_2/N ratio.³² Owing to the simple molecular structure of urea with fully oxidized carbon, volatile byproducts from chemical urea chlorination were almost exclusively chloramines.^{30,33} Although the appreciable chlorinated byproducts from RCS mediated urea oxidation were limited to ClO_3^- and NH_2Cl in this study, a wide array of organics present in human wastes pose a risk of toxicity from other chlorinated byproducts. The harmful byproducts potentially formed during electrochemical treatment of human wastes may limit the reusability of the effluent to non-potable purposes and require post-treatment units. Further investigation is necessary to identify the matrix of by-products and their toxicity in more realistic situations.

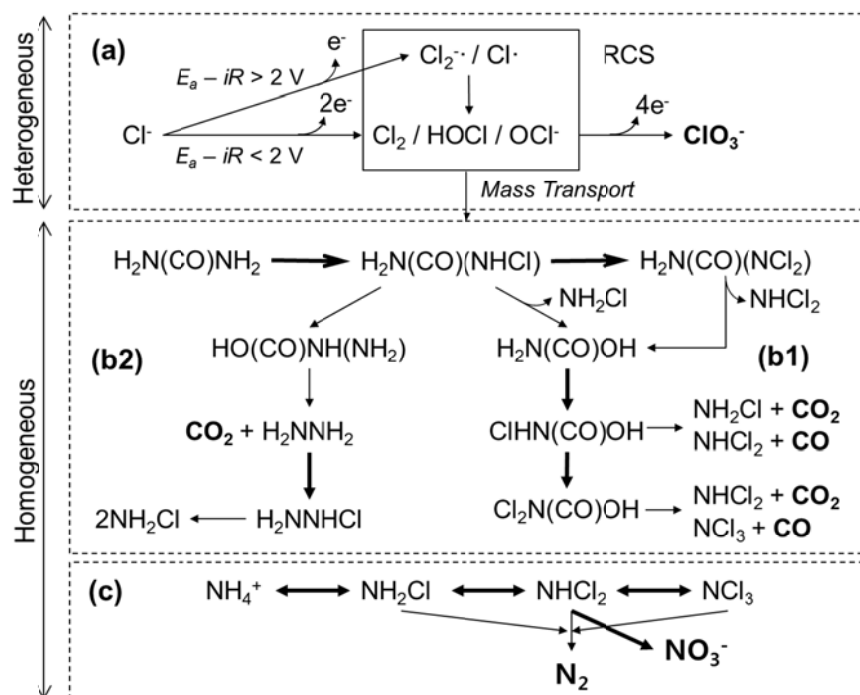


Figure 2.10. Proposed reaction pathways of urea degradation by electrochemically generated reactive chlorine species (RCS); (a) Cl^- oxidation on $\text{BiO}_x/\text{TiO}_2$ anode to produce RCS and ClO_3^- , (b1) chlorinated carbamic acids mediated chloramines and CO_2 (CO) generation, (b2) chlorinated hydrazine mediated chloramines and CO_2 generation, and (c) chloramine mediated N_2 and NO_3^- generation. Bold arrows in (b) and (c) represent redox reactions involving the RCS while the final products are specified in bold characters.

2.3.6. Urea Degradation Pathways. Based on the experimental findings, we propose reaction pathways between urea and electrochemically generated RCS as shown in Figure 2.10. The evolution of $[\text{Cl}_{\text{DPD}}]$ supports chloramines and chloramides as the reaction intermediates. The initial chlorination step appears to be the rate determining since the electron-withdrawing effects of substituted Cl would reduce the bond strength of neighboring amido hydrogen. The overall rate appears to be accelerated by chlorine radicals via hydrogen atom abstraction and rapid addition. A radical driven cleavage of carbonyl double bond or resonance stabilized C-N bond should be minimized in the

initial step, since the dominant carbon end product was observed to be CO₂. The dichlorourea or even monochlorourea will undergo rapid hydrolysis rather than further chlorine substitution,³⁴ via a pattern similar to base catalyzed haloform reaction, to produce mono-/di-chloramine and carbamic acid. Further chlorinations of the carboxylic intermediates produce more chloramines, CO₂ and presumably CO as a minor product. A generation of hydrazine by a Hoffmann rearrangement of monochlorourea is also feasible,⁶ where CO is unlikely to form. The inorganic chloramines undergo a breakpoint chlorination pathway to produce dominantly N₂ or further oxidation to NO₃⁻ with a lower yield.

2.4. SUPPORTING INFORMATION

2.4.1. Quantification of Molar Flow Rates of Gas Products. The m/z values of 14 and 44 were chosen as characteristic m/z for N₂ and CO₂, respectively. Potential interferences from CO₂, CO and N₂O prohibited the ion intensity of m/z 14 to be used for N₂ quantification. Based on the negligible signal at m/z 30, an interference of N₂O to the signal at m/z 44 was assumed to be marginal. The signal fraction of each characteristic m/z was calculated by the ratio to the sum of ion intensities (m/z 1 to 300). Based on the fragmentation profiles of standard N₂ and CO₂ provided by the supplier, the volume fractions were calculated by the following equations:

$$F_{N_2} = \frac{1080}{72} \frac{I_{14}}{\sum_1^{300} I_i} F_T \quad (\text{m/z } 28:14:29 = 1000:72:8) \quad (2.4)$$

$$F_{CO_2} = \frac{1199}{1000} \frac{I_{44}}{\sum_1^{300} I_i} F_T \quad (\text{m/z } 44:28:16 = 1000:114:85) \quad (2.5)$$

where, I_i is ion intensity of fragment m/z i , while F_{N_2} , F_{CO_2} , and F_T represent the molar flow rate of N_2 , CO_2 , and total gaseous products, respectively. F_T was calculated by converting the observed volumetric flow rate using ideal gas law, while considering conversion factors of the major gas components (1.4 for Ar, *ca.* 1 for H_2 , O_2 , N_2 , H_2O).

$$F_T = \left(\frac{X_{Ar}}{1.4} + \frac{1 - X_{Ar}}{1} \right)^{-1} \frac{P}{RT} Q_{obs} \quad (2.6)$$

where, X_{Ar} is the volumetric fraction of Ar, Q_{obs} is the observed volumetric flow rate of total gaseous products, P is the operational pressure (1 atm), R is the gas constant, and T is the operational temperature (293 K).

2.4.2. Measurement of Urea Concentration. Figure 2.11 shows the evolution of the urea concentration under variable current density conditions, which was measured by urease hydrolysis method.¹⁶ The measured urea concentration dropped off for the first sample under potential bias, whose further decrease was marginal. The required charge for the decrease in urea concentration for the initial 10 min exceeded the total passed charge, even when assuming one electron transfer for the urea transformation. The presence of reactive chlorine species (RCS), even with a trace concentration, would inhibit the activity of the enzyme urease.²⁰ In addition, the RCS was found to interfere in the spectrometric urea analysis by diacetylmonoxime.³⁵ The color generation by the reagent addition appeared to increase with the electrolysis time.

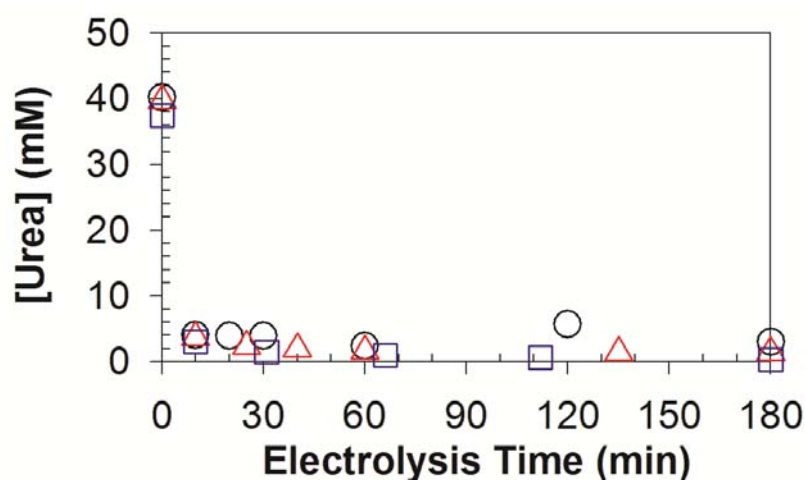


Figure 2.11. Time profiles of urea concentration during potentiostatic electrolysis of 41.6 mM urea solutions with 50 mM Cl^- (60 mL) as control; E_a : (circle) 2.2 V NHE in divided cell, (triangle) 3.0 V NHE in divided cell, (square) 3.0 V NHE in single compartment cell.

2.5. REFERENCES

- (1) Rollinson, A. N.; Jones, J.; Dupont, V.; Twigg, M. V. Urea as a hydrogen carrier: a perspective on its potential for safe, sustainable and long-term energy supply. *Energy & Environmental Science* **2011**, *4* (4), 1216-1224.
- (2) Maurer, M.; Pronk, W.; Larsen, T. A. Treatment processes for source-separated urine. *Water Research* **2006**, *40* (17), 3151-3166.
- (3) De Laat, J.; Feng, W. T.; Freyfer, D. A.; Dossier-Berne, F. Concentration levels of urea in swimming pool water and reactivity of chlorine with urea. *Water Research* **2011**, *45* (3), 1139-1146.
- (4) *Clean watersheds needs survey: report to congress*; EPA-832-R-10-002; United States Environmental Protection Agency: Washington, DC., 2008.; water.epa.gov/scitech/datait/databases/cwns/upload/cwns2008rtc.pdf.
- (5) Amstutz, V.; Katsaounis, A.; Kapalka, A.; Comninellis, C.; Udert, K. M. Effects of carbonate on the electrolytic removal of ammonia and urea from urine with thermally prepared IrO_2 electrodes. *Journal of Applied Electrochemistry* **2012**, *42* (9), 787-795.

- (6) Simka, W.; Piotrowski, J.; Robak, A.; Nawrat, G. Electrochemical treatment of aqueous solutions containing urea. *Journal of Applied Electrochemistry* **2009**, *39* (7), 1137-1143.
- (7) Hernlem, B. J. Electrolytic destruction of urea in dilute chloride solution using DSA electrodes in a recycled batch cell. *Water Research* **2005**, *39* (11), 2245-2252.
- (8) Kim, J.; Choi, W. J. K.; Choi, J.; Hoffmann, M. R.; Park, H. Electrolysis of urea and urine for solar hydrogen. *Catalysis Today* **2013**, *199*, 2-7.
- (9) Boggs, B. K.; King, R. L.; Botte, G. G. Urea electrolysis: direct hydrogen production from urine. *Chemical Communications* **2009**, (32), 4859-4861.
- (10) Vedharathinam, V.; Botte, G. G. Understanding the electro-catalytic oxidation mechanism of urea on nickel electrodes in alkaline medium. *Electrochimica Acta* **2012**, *81*, 292-300.
- (11) Yan, W.; Wang, D.; Botte, G. G. Electrochemical decomposition of urea with Ni-based catalysts. *Applied Catalysis B-Environmental* **2012**, *127*, 221-226.
- (12) Jara, C. C.; Di Giulio, S.; Fino, D.; Spinelli, P. Combined direct and indirect electrooxidation of urea containing water. *Journal of Applied Electrochemistry* **2008**, *38* (7), 915-922.
- (13) Simka, W.; Piotrowski, J.; Nawrat, G. Influence of anode material on electrochemical decomposition of urea. *Electrochimica Acta* **2007**, *52* (18), 5696-5703.
- (14) Blatchley, E. R.; Cheng, M. M. Reaction mechanism for chlorination of urea. *Environmental Science & Technology* **2010**, *44* (22), 8529-8534.
- (15) Cho, K.; Qu, Y.; Kwon, D.; Zhang, H.; Cid, C. A.; Aryanfar, A.; Hoffmann, M. R. Effects of anodic potential and chloride ion on overall reactivity in electrochemical reactors designed for solar-powered wastewater treatment. *Environmental Science & Technology* **2014**, *48* (4), 2377-2384.
- (16) Cho, K.; Kwon, D.; Hoffmann, M. R. Electrochemical treatment of human waste coupled with molecular hydrogen production. *Rsc Advances* **2014**, *4* (9), 4596-4608.
- (17) Bergmann, M. E. H.; Koparal, A. S. Studies on electrochemical disinfectant production using anodes containing RuO₂. *Journal of Applied Electrochemistry* **2005**, *35* (12), 1321-1329.

- (18) Wilsenach, J. A.; Schuurbijs, C. A. H.; van Loosdrecht, M. C. M. Phosphate and potassium recovery from source separated urine through struvite precipitation. *Water Research* **2007**, *41* (2), 458-466.
- (19) Revilla, M.; Alexander, J.; Glibert, P. M. Urea analysis in coastal waters: comparison of enzymatic and direct methods. *Limnology and Oceanography-Methods* **2005**, *3*, 290-299.
- (20) Ikematsu, M.; Kaneda, K.; Iseki, M.; Yasuda, M. Electrochemical treatment of human urine for its storage and reuse as flush water. *Science of the Total Environment* **2007**, *382* (1), 159-164.
- (21) Shang, C.; Gong, W. L.; Blatchley, E. R. Breakpoint chemistry and volatile byproduct formation resulting from chlorination of model organic-N compounds. *Environmental Science & Technology* **2000**, *34* (9), 1721-1728.
- (22) Jafvert, C. T.; Valentine, R. L. Reaction scheme for the chlorination of ammoniacal water. *Environmental Science & Technology* **1992**, *26* (3), 577-586.
- (23) Kapalka, A.; Katsaounis, A.; Michels, N. L.; Leonidova, A.; Souentie, S.; Comminellis, C.; Udert, K. M. Ammonia oxidation to nitrogen mediated by electrogenerated active chlorine on Ti/PtO_x-IrO₂. *Electrochemistry Communications* **2010**, *12* (9), 1203-1205.
- (24) Bunce, N. J.; Bejan, D. Mechanism of electrochemical oxidation of ammonia. *Electrochimica Acta* **2011**, *56* (24), 8085-8093.
- (25) Deborde, M.; von Gunten, U. Reactions of chlorine with inorganic and organic compounds during water treatment - Kinetics and mechanisms: A critical review. *Water Research* **2008**, *42* (1-2), 13-51.
- (26) Park, H.; Vecitis, C. D.; Hoffmann, M. R. Electrochemical water splitting coupled with organic compound oxidation: The role of active chlorine species. *Journal of Physical Chemistry C* **2009**, *113* (18), 7935-7945.
- (27) Neta, P.; Huie, R. E.; Ross, A. B. Rate constants for reactions of inorganic radicals in aqueous-solution. *Journal of Physical and Chemical Reference Data* **1988**, *17* (3), 1027-1284.
- (28) Kim, K. W.; Kim, Y. J.; Kim, I. T.; Park, G. I.; Lee, E. H. Electrochemical conversion characteristics of ammonia to nitrogen. *Water Research* **2006**, *40* (7), 1431-1441.

- (29) Peez, G.; Saiz, J.; Ibanez, R.; Urtiaga, A. M.; Ortiz, I. Assessment of the formation of inorganic oxidation by-products during the electrocatalytic treatment of ammonium from landfill leachates. *Water Research* **2012**, *46* (8), 2579-2590.
- (30) Li, J.; Blatchley, E. R. Volatile disinfection byproduct formation resulting from chlorination of organic-nitrogen precursors in swimming pools. *Environmental Science & Technology* **2007**, *41* (19), 6732-6739.
- (31) Judd, S. J.; Bullock, G. The fate of chlorine and organic materials in swimming pools. *Chemosphere* **2003**, *51* (9), 869-879.
- (32) Weaver, W. A.; Li, J.; Wen, Y. L.; Johnston, J.; Blatchley, M. R.; Blatchley, E. R. Volatile disinfection by-product analysis from chlorinated indoor swimming pools. *Water Research* **2009**, *43* (13), 3308-3318.
- (33) Schmalz, C.; Frimmel, F. H.; Zwiener, C. Trichloramine in swimming pools - Formation and mass transfer. *Water Research* **2011**, *45* (8), 2681-2690.
- (34) Chattaway, F. D. The action of chlorine upon urea whereby a dichloro urea is produced. *Proceedings of the Royal Society of London Series a-Containing Papers of a Mathematical and Physical Character* **1908**, *81* (549), 381-388.
- (35) Prescott, L. M.; Jones, M. E. Modified methods for determination of carbamyl aspartate. *Analytical Biochemistry* **1969**, *32* (3), 408-419.